Calculating Optical Rotatory Dispersion Spectra in Solution Using a Smooth Dielectric Model

J. Coleman Howard and T. Daniel Crawford*

Department of Chemistry, Virginia Tech, Blacksburg, VA 24061, USA

E-mail: crawdad@vt.edu

Abstract

The calculation of specific rotation of molecules in solution is probed at the coupled cluster (CC) level utilizing a continuum dielectric model based on a definition of the dielectric permittivity as a smooth function of electron density. Solvation effects are captured through polarization of Hartree-Fock (HF) molecular orbitals before subsequent calculations with the coupled cluster singles and doubles (CCSD) method. For the challenging (S)-methyloxirane molecule, CCSD specific rotations yield an incorrect sign for the rotation in water, and the continuum model is unable to predict the wide variations in the optical rotatory dispersion (ORD) curves seen for nonpolar solvents of similar dielectric constant. In two molecules, $(1S,4S)$-norbornenone and (S)-2-chloropropionitrile, specific rotations computed with CCSD in conjunction with implicit solvent fail to provide solvent shifts of the correct order of magnitude, indicating that the solvent response is a major contribution to the overall solvation effect.

1 Introduction

Successfully modeling chiroptical properties such as optical rotation ostensibly requires the same theoretical considerations involved in modeling any molecular property, e.g., choices in atomic orbital (AO) basis sets and approaches to electron correlation effects. Optical rotation calculations, however, demonstrate a particular sensitivity to these theoretical details and others, including the treatment of the environment surrounding a chiral molecule, and represent an ongoing challenge to theoretical quantum chemistry.[1–3] Highly correlated quantum mechanical (QM) methods[4–6] offer the most reliable means of calculation, however even an accurate correlated method such as the coupled cluster singles and doubles (CCSD) method can produce specific rotation values significantly at odds with experimental results. One difficulty in comparing accurate QM wavefunction methods with experiment is that especially large, flexible AO basis sets are needed to obtain converged optical rotation values near the complete basis set (CBS) limit,[7–9] and, in contrast to many molecular properties,[10] diffuse basis functions are of critical importance in optical rotation calculations.[7,11,12] Even with a sufficient treatment of dynamical electron correlation and a basis set approaching the CBS limit, a single optical rotation calculation on a molecular system in its minimum-energy geometry may be an inappropriate comparison to an experimental value. For example, it is known that vibrational corrections to specific rotation can be significant,[13–18] even to the extent that the molecular vibrations induce sign changes at points in the optical rotatory dispersion (ORD) curve.[14] For conformationally flexible molecules, a great number of conformations may need to be considered depending on the experimental conditions.[19–22]

In addition to these factors, the role of solvent is understood to be of primary importance in ORD spectra.[23,24] The specific rotation of a molecule measured in the gas phase can differ drastically from the rotation in solution or the condensed phase, even changing sign depending on the solvent.[23,25] In contrast to many other properties where nonpolar solvent environments are expected to more closely mimic conditions in the gas phase relative to polar solvents, the opposite can be true for measured specific rotations.[25] An additional

complication in modeling rotation in solution is that the structure of the surrounding solvent molecules itself may also contribute to specific rotation, as the "chiral imprint" can be responsible for a significant portion of the solvent shift.[26,27] A more complete understanding of the nature of these solvent effects is essential to increasing the reliability of theoretical optical rotation predictions across all phases.

Solvent effects have been incorporated into optical rotation calculations often with an implicit solvation approach, such as the venerable polarizable continuum model (PCM).[28,29] Often used in conjunction with density functional theory (DFT) methods, DFT/PCM treatments have yielded mixed results in specific rotation calculations in comparison to experimental values.[16,30,31] An explicit treatment of solvent molecules has the advantage of capturing specific solute-solvent interactions inaccessible to a continuum model, (e.g., hydrogen bonding). The inclusion of explicit solvent effects has contributed valuable insight into the role of solvent molecules in methyloxirane's optical rotation, probing the contributions of the dissymmetric solvent structure,[26,27] as well as achieving quantitative agreement with experimental measurements in water when combined with an implicit treatment of the bulk solvent and vibrational corrections.[32] Unfortunately, explicit solvation treatments require extensive sampling of configurations, and typically thousands of molecular dynamics snapshots are needed for converged results.[26,27,32] The associated computational cost of of such an approach necessarily limits the applicability of most wavefunction-based electronic structure methods, and one often relies on DFT methods, where gas-phase specific rotation results, for methyloxirane in particular, depend on significant error cancellation to obtain correct signs.[33] In this work, we investigate the combination of coupled-cluster linear response theory and an implicit solvation model based on a smooth definition of the dielectric permittivity to obtain specific rotation values in solution.

The implicit solvent model utilized herein is based on a definition of the dielectric permittivity as a function of electron density. Introduced by Fattebert and Gygi,[34,35] this model was developed for use in the context of plane-wave based DFT calculations[36–40] and has been

particularly successful in computing accurate solvation energies relative to contemporary solvent models.[38,39] The definition of the dielectric permittivity takes the form of Equation 1.

$$\epsilon[\rho(\mathbf{r})] = 1 + \frac{\epsilon_\infty - 1}{2}\left[1 + \frac{1 - (\rho(\mathbf{r})/\rho_0)^{2\beta}}{1 + (\rho(\mathbf{r})/\rho_0)^{2\beta}}\right] \tag{1}$$

In this model, the dielectric permittivity ϵ is determined by the electron density (ρ) and depends on the two parameters ρ_0 and β, which control the transition of ϵ from the vacuum value of one to the dielectric constant of the bulk solvent ϵ_∞. The appropriate electrostatic problem in this case corresponds to solving the generalized Poisson equation (GPE) (Equation 2) for the electrostatic potential (V^{GPE}).

$$\nabla \cdot \left[\epsilon(\mathbf{r})\nabla V^{\mathrm{GPE}}(\mathbf{r})\right] = -4\pi\rho_{\mathrm{tot}}(\mathbf{r}) \tag{2}$$

Unlike the standard Poisson equation corresponding to electrostatics in vacuum or a homogeneous permittivity, which can be solved analytically, the GPE in Equation 2 must in general be solved by numerical techniques. Its solution here is achieved by interfacing with DL_MG,[41] an open-source multigrid solver library. As previously described,[42] real-space grid representations of the permittivity and total density ρ_{tot} are used to obtain V^{GPE}, which is numerically integrated into the AO basis and iterated to self-consistency along with the HF molecular orbitals. We have previously[42] incorporated this continuum solvent model in a Hartree-Fock framework to extend its use to correlated wavefunction methods. A study of small molecules with well-known electronic excitation solvent shifts demonstrated good performance for this solvation model in conjunction with the EOM-CCSD method, typically reproducing experimentally determined n$\rightarrow \pi^*$ blue shifts to within 0.1 eV.[42] This continuum dielectric model requires only two parameters and, capturing the effects of solvation through

the molecular orbitals and Fock matrix elements (analogous to a PTE approximation in PCM),[43,44] can be readily extended to any post-HF correlated method. This approach can be contrasted with a more complete treatment of continuum solvation at the correlated level, which would include the solvent's response to electron correlation and/or the electric and magnetic field perturbations, as well as a proper consideration of non-equilibrium solvation effects, as has been demonstrated by Caricato.[45] Despite the present model's relative simplicity, excitation energies computed via EOM-CCSD calculations in solution have compared favorably with those resulting from more sophisticated approaches.[42] In this work, we apply this smooth dielectric model (hereafter, referred to as the FGS model) to the computation of specific rotations in solution at the CCSD level.

2 Computational Methods

Specific rotation values were computed with the CCSD method for three molecules, (S)-methyloxirane, $(1S,4S)$-norbornenone, and (S)-2-chloropropionitrile using the aug-cc-pVDZ basis set.[46] Each of these calculations utilize the velocity-gauge representation of the dipole operator, ensuring origin-independent results, and all reported specific rotation values represent modified velocity-gauge results.[47] Each of these geometries was optimized with the B3LYP DFT functional using the 6-311G(d,p) basis set.[48] The core orbitals (i.e., $1s$ for C,N, and O; $1s2s2p$ for Cl) were kept frozen in the CCSD energy and response calculations. In defining the dielectric permittivity according to Equation 1, the solvent cavity was fixed based on a converged electronic SCF density computed in vacuum, as in Reference 42. For selecting the dimensions of the real-space grid used in solving the GPE for the electrostatics in solution, the number of points and grid spacing were selected such that specific rotations computed in vacuum with electrostatic computed from the GPE reproduced those from a conventional CCSD specific rotation calculation. For the three molecules studied here, the maximum deviation between those rotation values is less than 4 deg dm^{-1} (g/mL)$^{-1}$, and

corresponds to the specific rotation of $(1S,4S)$-norbornenone at 355 nm, which has a magnitude greater than 3000 deg dm^{-1} (g/mL)$^{-1}$. The values of the electrostatic potential on the boundary points of the grid are approximated by computing the potential associated with a homogeneous medium of ϵ corresponding to the solvent's dielectric constant, as in previous works.[38,42] The grid details, as well as parameters used in the DL_MG multigrid calculations, are provided in the Supporting Information. For the PCM calculations performed here, geometry optimizations were performed with Gaussian09 software.[49] All other computations were performed with the Psi4 software package,[50] utilizing an interface to PCMSolver[51] for specific rotation calculations with PCM solvents. Those calculations utilized PCM cavities constructed with Bondi radii scaled by a factor of 1.2.

3   Results and Discussion

Table 1: Specific rotations (deg dm^{-1} (g/mL)$^{-1}$) of (S)-methyloxirane computed in vacuum and shifts computed in solvents at the CCSD/aug-cc-pVDZ level

λ (nm)	Vacuum $[\alpha]_\omega$	C$_6$H$_{12}$ $\Delta[\alpha]_\omega$	CCl$_4$ $\Delta[\alpha]_\omega$	C$_6$H$_6$ $\Delta[\alpha]_\omega$	CH$_3$CH$_2$OH $\Delta[\alpha]_\omega$	CH$_3$CN $\Delta[\alpha]_\omega$	H$_2$O $\Delta[\alpha]_\omega$
253	104.2	-1.6	-0.8	-0.6	+41.2	+47.9	+63.1
302	-42.8	+11.5	+13.3	+13.6	+52.0	+56.5	+66.2
365	-59.3	+10.1	+11.5	+11.8	+38.6	+41.4	+47.5
436	-50.1	+7.5	+8.5	+8.7	+27.2	+29.0	+33.0
546	-35.2	+4.9	+5.5	+5.6	+17.1	+18.2	+20.7
578	-31.9	+4.3	+4.9	+5.0	+15.2	+16.2	+18.4
589	-30.9	+4.2	+4.7	+4.8	+14.7	+15.6	+17.6

The case of methyloxirane perhaps best exemplifies the large role solvent effects can play in optical rotation. Since the work of Kumata *et al.*,[23] it has been recognized that the solvent environment has a significant effect on the ORD curve of methyloxirane. These and subsequent experiments have revealed qualitatively different shapes for the ORD curves in benzene compared to those in polar solvents water and acetonitrile.[23,25] At a wavelength of 302 nm, the specific rotation of (S)-methyloxirane in benzene is nearly -100 deg dm^{-1} (g/mL)$^{-1}$, while, in water, the measured rotation is around +60 deg dm^{-1} (g/mL)$^{-1}$.[25] Specific rotations measured at several wavelengths on the ORD curve for a variety of other solvents produce a range of rotation values intermediate between these two solvents,[23,25] and available gas-phase measurements lie closer to those in more polar solvents in this case.[25]

A variety of computational efforts have addressed the problem of methyloxirane's specific rotation in solvent. Mennucci *et al.*[30] examined solvent effects on the rotation of several molecules, including methyloxirane, presenting the first demonstration of electronic structure calculations of optical rotation to employ PCM to model the solvent environment. Despite the success of PCM in modeling a variety of molecular properties,[29] B3LYP[52–54] PCM calculations were incapable of reproducing the experimental ordering of specific rotations in different solvents. B3LYP PCM calculations have also been combined with zero-point vi-

brational corrections in methyloxirane,[16] resulting in improvements in the computed solvent shifts in cyclohexane relative to experiment. For more polar solvents, however, that methodology was unable to model the correct relative shifts observed experimentally. Beyond density functional theory, optical rotation of methyloxirane in solution has also been investigated at the coupled-cluster level, including correlation up to an approximation of triple excitations in the CC3 method.[55] In conjunction with a spherical cavity dielectric model in CC/DC computations,[55] those highly correlated methods also failed to predict the observed trends across a variety of solvents.

Table 1 summarizes the results of CCSD/aug-cc-pVDZ specific rotation values of (S)-methyloxirane computed in vacuum, as well as in a variety of solvents treated as a continuum dielectric. The wavelengths in the first column cover a range of values for which experimental measurements are available. The CCSD/aug-cc-pVDZ specific rotation values for the isolated molecule are given by the second column of Table 1. At 253 nm, the vacuum rotation value is +104.2 deg dm^{-1} (g/mL)$^{-1}$, becoming more negative at -59.3 deg dm^{-1} (g/mL)$^{-1}$ as the wavelength increases to 365 nm. At longer wavelengths, the vacuum rotation remains negative, reaching -30.9 deg dm^{-1} (g/mL)$^{-1}$ at 589 nm. The remaining columns of Table 1 give the solvent shifts computed with the FGS model in combination with CCSD response calculations, relative to the CCSD vacuum rotations. For the nonpolar solvents cyclohexane, carbon tetrachloride, and benzene (third through fifth columns), the predicted shifts are on the order of several deg dm^{-1} (g/mL)$^{-1}$. The large positive rotation at 253 nm is shifted only slightly smaller in each of these solvents, and none of the shifts exceed 2 deg dm^{-1} (g/mL)$^{-1}$. The negative specific rotations near 300 nm all undergo larger shifts towards more positive values in the nonpolar environments, the magnitude of these shifts ranging from +4 to +14 deg dm^{-1} (g/mL)$^{-1}$, with the largest shifts due to the rotations calculated at 302 nm and 365 nm. For the three polar solvents considered here (ethanol, acetonitrile, and water), the specific rotation shifts relative to vacuum CCSD values are much larger. At all wavelengths, the shifts are positive (last three columns of 1). The predicted specific rotation shifts in

9

water at 253 nm and 302 nm exceed +60 deg dm^{-1} (g/mL)$^{-1}$, a shift which is larger than the magnitude of any of the negative vacuum specific rotation values above 300 nm.
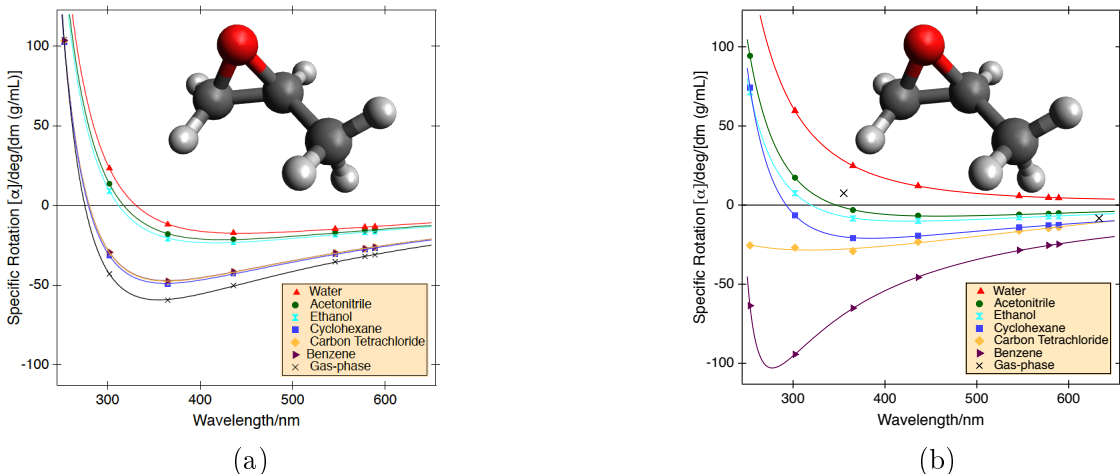

Figure 1: Optical rotatory dispersion curves of (S)-methyloxirane (a) computed at the CCSD/aug-cc-pVDZ level with various solvents and (b) from experimentally determined values[25]

Figure 1 displays the ORD curves for (S)-methyloxirane in various solvents, including those computed at the CCSD/aug-cc-pVDZ level in implicit solvent with the FGS model in Figure 1(a) and from experimental determinations in Figure 1(b).[25] The experimental rotation values display a wide range across all solvents, with the most polar solvents (water and acetonitrile) showing positive rotations above 50 deg dm^{-1} (g/mL)$^{-1}$ at wavelengths below 300 nm. In benzene, the rotation of (S)-methyloxirane shifts to nearly -100 deg dm^{-1} (g/mL)$^{-1}$ in the same wavelength range experimentally. Comparing the CCSD/aug-cc-pVDZ specific rotations computed in solution using the smooth FGS model (Figure 1(a)), the relative ordering of the polar solvents water, acetonitrile, and ethanol is correct, and the computed ORD curves display a qualitative agreement with experiment for most of the polar solvents. However, there are clearly major discrepancies in the calculated and experimental curves. For example, the experimental ORD curve of (S)-methyloxirane in water is positive at all wavelengths, while the values computed here predict negative rotations above 302 nm. For the remaining solvents, the sign of the rotation is correctly predicted, although the actual values can deviate significantly from experiment, such as in benzene, where the computed

rotation value is too large at 302 nm by more than 60 deg dm^{-1} (g/mL)$^{-1}$. In addition, because of the similar dielectric constants of the nonpolar solvents here, the implicit solvent calculations are unable to predict the variations seen experimentally among the ORD curves in nonpolar solvents.

In evaluating the quality of the CCSD calculations with the FGS model, the shifts relative to vacuum are perhaps the most important, since the absolute specific rotations in solution may benefit from error cancellation in regards to basis set incompleteness, a lack of vibrational corrections, etc. The experimental vacuum values[25] are 7.49 deg dm^{-1} (g/mL)$^{-1}$at 355 nm and -8.39 deg dm^{-1} (g/mL)$^{-1}$at 633 nm (marked with black X's in Figure 1). The CCSD/aug-cc-pVDZ vacuum values, on the other hand, are represented by the most negative computed ORD curve. At these two points, then, almost all of the computed shifts in Table 1 are in the wrong direction, with only the calculations in water solvent correctly predicting positive shifts in the rotation. The unsatisfactory performance of the CCSD shifts computed with the FGS model are in line with previous efforts to apply continuum solvation to the problem of methyloxirane's rotation in solution. The B3LYP PCM shifts computed at 589 nm by Mennucci *et al.*[30] agree with the CCSD FGS computed shifts for the nonpolar solvents to within 2 deg dm^{-1} (g/mL)$^{-1}$, while the acetonitrile shift computed in this work are a bit more positive (by +8 deg dm^{-1} (g/mL)$^{-1}$). Solvents shifts at 355 nm, also with B3LYP and PCM, were reported by Kongsted *et al.*[16] and a similar shift was seen to that computed here at 365 nm in cyclohexane, while the CCSD FGS results again predict larger shifts in polar solvents compared to a DFT with PCM approach. Importantly, Kongsted *et al.* noted the importance of vibrational contributions to the shifts themselves, as the effect was large enough in the case of cyclohexane to change the sign of the computed shift at long wavelengths.[16] In contrast to the present CCSD results with the FGS model, a previous attempt to model the solvents with a continuum model at the CCSD level[33] utilizing the CC/DC model predicts small, negative shifts in the specific rotations of (S)-methyloxirane at 355 nm for the nonpolar solvents examined here, in better accord with the experimental

11

picture and likely an improvement due to the CC/DC approach incorporating the response of the solvent environment into the CC response equations.[56]
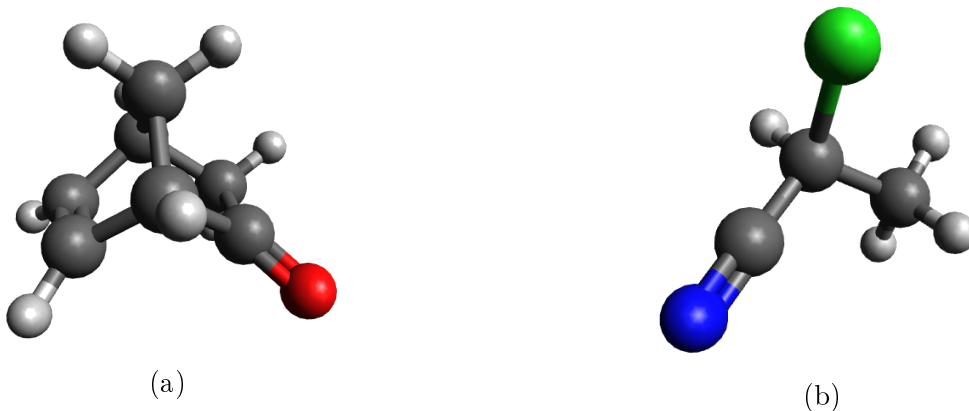

(a)

(b)

Figure 2: Two molecules studies in this work: (a) (*1S,4S*)-norbornenone and (b) (*S*)-2-chloropropionitrile

Norbornenone is a molecule which has attracted theoretical interest due to its very large-magnitude specific rotation values relative to structurally similar chiral molecules.[7,31,57–60] The especially large rotation value has been analyzed in terms of the excited state contributions,[60] as well as the contributions from specific localized orbitals, and the lowest excited state appears to be largely responsible for the sizable rotation,[60] with a favorable alignment of the carbonyl and alkenyl groups playing a significant role.[59,60] Modeling the specific rotation of the isolated norbornenone molecule has been a challenge and shows a strong dependence on theoretical method. DFT[31,57–60] and CC calculations[7,31,58] provide vastly different rotation values, and at 355 nm, the experimental value of -6310 deg dm^{-1} (g/mL)$^{-1}$ is between B3LYP and CCSD results, which both deviate from experiment by more than 2000 deg dm^{-1} (g/mL)$^{-1}$.[31]

Norbornenone also undergoes a significant solvation effect, which is under investigation here. Table 2 provides the calculated CCSD/aug-cc-pVDZ vacuum rotations and shifts computed with the FGS continuum treatment of solvent effects. For additional comparison, the results of a B3LYP PCM treatment of implicit solvation have been included as well.[31] For the large negative rotation at 355 nm, the CCSD FGS implementation predicts shifts

12

Table 2: Specific rotations (deg dm^{-1} (g/mL)$^{-1}$) of (*1S,4S*)-norbornenone computed in vacuum and shifts computed in solvents at the CCSD/aug-cc-pVDZ level

		CCSD		PCM-B3LYP[a]		Experiment[a]	
	Vacuum	C_6H_{12}	CH_3CN	C_6H_{12}	CH_3CN	C_6H_{12}	CH_3CN
λ (nm)	$[\alpha]_\omega$	$\Delta[\alpha]_\omega$	$\Delta[\alpha]_\omega$	$\Delta[\alpha]_\omega$	$\Delta[\alpha]_\omega$	$\Delta[\alpha]_\omega$	$\Delta[\alpha]_\omega$
355	-3732.2	+44.6	+131.8	-1066	-855	-2849	-2297
436	-1429.4	-4.9	-15.0	–	–	–	–
589	-551.7	-5.5	-16.8	-152	-118	-226	-195
633	-454.5	-4.8	-14.9	-125	-96	-182	-159

[a] Reference 31

in the positive direction for both cyclohexane and acetonitrile solvents. Comparing to the experimentally determined shifts in the last two columns of Table 2, these computed shifts are an order of magnitude smaller than experiment, and the CCSD FGS results predict a shift in the wrong direction. For the two rotation values that have been measured in these solvents at 589 nm and 633 nm, the CCSD FGS calculations predict the correct direction of the shifts, but again the magnitudes are an order of magnitude too small. The previously reported[31] solvents shifts of norbornenone using B3LYP in conjunction with the PCM model perform significantly better in regards to experiment. The PCM shifts predicted in cyclohexane and acetonitrile are still underestimated with respect to the measured shifts, but they are of the correct order of magnitude at each wavelength, and the cyclohexane shifts are correctly predicted to be larger in each case.

Because the calculated optical rotations in norbornenone are so dependent on the theoretical method, it is difficult to determine the source of the poor performance of the implicit model used here without continuum dielectric calculations performed at a level comparable to CCSD. In order to further investigate shortcomings of the CCSD implementation of the FGS model for optical rotation, we have performed specific rotation calculations of (*S*)-2-chloropropionitrile, for which recent experimental measurements and CCSD-PCM computed rotations have been obtained by Aharon *et al.*[61] Table 3 gives the vacuum CCSD/aug-cc-pVDZ specific rotation values along with solvent shifts computed here with the FGS model,

the CCSD-PCM/aug-cc-pVDZ reported shifts, and those from experiment.[61] For the vacuum values in the first column of data in Table 3, we note that the CCSD/aug-cc-pVDZ vacuum values for (S)-2-chloropropionitrile are in very good agreement with the experimental values[61] of -37.9 deg dm^{-1} (g/mL)$^{-1}$, -18.5 deg dm^{-1} (g/mL)$^{-1}$, -8.1 deg dm^{-1} (g/mL)$^{-1}$, and -6.8 deg dm^{-1} (g/mL)$^{-1}$ at the wavelengths reported in the table. As with norbornenone, the CCSD method in conjunction with the FGS model significantly underestimates the specific rotation shift at each wavelength. The CCSD-PCM computed shifts reported in Table 3 do not include the zero-point vibrational corrections reported in Reference 61 because we are interested in the most straightforward comparison with the CCSD results computed here to understand the drastically underestimated shifts. Even without the zero-point vibrational corrections, which in most cases improve the CCSD-PCM shifts relative to experiment, the solvent effects on the optical rotation of (S)-2-chloropropionitrile appear to be well described by CCSD-PCM, with the computed shifts always in the right direction and typically within a few deg dm^{-1} (g/mL)$^{-1}$ of experimental values. To understand the failure of the CCSD shifts computed with the FGS model, we have performed additional PCM computations to investigate whether the differences can be attributed to solute geometric effects, differences in the implicit models' cavity definitions, or the solvent response treatment.

In Table 4, the CCSD/aug-cc-pVDZ shifts computed using the FGS model are compared to different computational protocol utilizing CCSD in conjunction with PCM. For these PCM computations, the PTE approximation is employed in the same manner as the FGS calculations. In other words, the effect of the implicit solvent is only captured through the polarization of the HF molecular orbitals, as well as the Fock matrix elements. In addition, the CCSD-PCM-PTE specific rotation calculations were performed on (S)-2-chloropropionitrile geometries optimized in vacuum, as well as in the corresponding solvent using PCM (2nd and 3rd columns of data in Table 4). Comparing the first two columns of data in Table 4, the CCSD-PCM-PTE cyclohexane shifts computed with the vacuum- optimized geometry are seen to be very close to those from the FGS model and, in fact, are slightly smaller than

14

the FGS shifts. The acetonitrile PCM-PTE shifts are of slightly larger magnitude relative to FGS using the vacuum geometry. Examining the CCSD-PCM-PTE shifts computed with PCM optimized geometries in the third column of data in Table 4, the effect of geometry is seen to have a minimal impact on the computed shifts. Capturing the solvent effects at the Hartree-Fock level in the PTE approximation and, thus, neglecting the solvent response to the electric and magnetic field perturbations results in a significant underestimation of the solvent's role in the specific rotation of (S)-2-chloropropionitrile, as evidenced by the shifts computed with the fully coupled linear response CCSD-PCM-PTED shifts from Reference 61 (last column of Table 4), which are an order of magnitude larger than each of the CCSD-PCM-PTE cyclohexane shifts. This is reminiscent of the situation for frozen-density embedding (FDE) potentials for modeling water solvent molecules in CC2 specific rotation calculations.[62] As with the CCSD FGS calculations performed here, capturing the solvent effects through FDE potentials incorporated into the Hartree-Fock reference state proved inadequate for reproducing the results from explicit solvent calculations due to the lack of solvent response. Unfortunately, a fully coupled implementation of a coupled-cluster linear response (LR) scheme including implicit solvent results in eight sets of coupled linear equations for perturbed CC t and λ amplitudes and a significantly higher computational cost. Recently introduced approximate schemes[63] for including solvent response in the CC-LR equations may offer a great advantage over PTE-type solvent treatments at a reduced computational effort.[63]

Table 3: Specific rotations (deg dm^{-1} (g/mL)$^{-1}$) of (S)-2-chloropropionitrile computed in vacuum and shifts computed in solvents at the CCSD/aug-cc-pVDZ level

	Vacuum	CCSD				CCSD-PCM[a,b]				Experiment[a]			
		C_6H_{12}	CH_3CN	$C_8H_{18}O$	CH_3OH	C_6H_{12}	CH_3CN	$C_8H_{18}O$	CH_3OH	C_6H_{12}	CH_3CN	$C_8H_{18}O$	CH_3OH
λ(nm)	$[\alpha]_\omega$	$\Delta[\alpha]_\omega$	$\Delta[\alpha]_\omega$	$\Delta[\alpha]_\omega$	$\Delta[\alpha]_\omega$	$\Delta[\alpha]_\omega$	$\Delta[\alpha]_\omega$	$\Delta[\alpha]_\omega$	$\Delta[\alpha]_\omega$	$\Delta[\alpha]_\omega$	$\Delta[\alpha]_\omega$	$\Delta[\alpha]_\omega$	$\Delta[\alpha]_\omega$
355	-27.6	-1.5	-0.7	-2.0	-0.8	-15.7	-10.9	-12.8	-10.2	-26.5	-7.5	-21.8	-14.2
437	-15.4	-0.9	-0.7	-1.4	-0.7	-9.4	-6.6	-7.6	-6.2	-17.8	-6.4	-15.1	-10.4
589	-7.3	-0.5	-0.4	-0.8	-0.5	-4.4	-3.0	-3.5	-2.8	-9.3	-3.5	-7.9	-6.0
633	-6.2	-0.4	-0.4	-0.7	-0.4	-3.9	-2.7	-3.1	-2.5	-7.8	-3.1	-6.9	-5.1

[a] Reference 61

[b] Zero-point vibrational corrections removed from reported CCSD-PCM shift

Table 4: CCSD/aug-cc-pVDZ specific rotations solvents shifts of (S)-2-chloropropionitrile computed with the FGS model and PCM continuum models

λ (nm)	$^{\text{vacuum}}_{\text{geom}}\Delta[\alpha]^{\text{FGS}}_{\omega}$	$^{\text{vacuum}}_{\text{geom}}\Delta[\alpha]^{\text{PCM}-\text{PTE}}_{\omega}$	$^{\text{solvent}}_{\text{geom}}\Delta[\alpha]^{\text{PCM}-\text{PTE}}_{\omega}$	$^{\text{solvent}}_{\text{geom}}\Delta[\alpha]^{\text{PCM,ab}}_{\omega}$
		Cyclohexane		
355	-1.5	-0.9	-1.0	-15.7
437	-0.9	-0.6	-0.6	-9.4
589	-0.5	-0.3	-0.3	-4.4
633	-0.4	-0.3	-0.3	-3.9
		Acetonitrile		
355	-0.7	-3.0	-2.7	-10.9
437	-0.7	-2.0	-1.6	-6.6
589	-0.4	-1.1	-0.8	-3.0
633	-0.4	-0.9	-0.7	-2.7

[a]Reference 61

[b] Zero-point vibrational corrections removed from reported shift

4 Conclusions

A dielectric continuum model based on a definition of the dielectric permittivity as a smooth function of the electron density was applied to the calculation of specific rotation at the CCSD level for molecules in solution. For (S)-methyloxirane, the computed ORD curves for most of the polar solvents are qualitatively in agreement with experimental measurements, but the CCSD results with the FGS solvent model failed to predict the correct positive sign of the molecule in water. Furthermore, the implicit model was unable to correctly predict the experimentally observed variation in nonpolar solvents with comparable dielectric constants. The failure of the smooth implicit model considered here in conjunction with CCSD is in line with previous attempts to model the specific rotation for methyloxirane in solution at lower levels of theory, and it appears an explicit consideration of specific solute-solvent interactions may be unavoidable for accurately modeling these effects.

In two other chiral molecules considered here, ($1S,4S$)-norbornenone and (S)-2-chloropropionitrile, CCSD specific rotations computed in solution via the FGS continuum model not only failed to satisfactorily reproduce the solvent shifts seen in experiment, but also demonstrated poor performance relative to contemporary continuum solvent models, in particular the fully coupled CCSD-PCM method. Previously applied to computing excitation energies in solution with success at the EOM-CCSD level, the failure of the CCSD FGS calculations here is attributed to the lack of solvent response in the PTE-like treatment of the solvent for post-HF calculations. Similar observations have been made when incorporating solvent effects through embedding potentials, and the specific rotations computed here demonstrate that the contribution of solvent response may be large enough at times to account for the majority of observed specific rotation solvent shifts.

Supporting Information Available

Optimized geometries of solute structures and summaries of grid parameterizations and solvents utilized in calculations.

5 Acknowledgments

References

(1) Crawford, T. D. *Ab Initio* Calculation of Molecular Chiroptical Properties. *Theor. Chem. Acc.* **2006**, *115*, 227–245.

(2) Srebro-Hooper, M.; Autschbach, J. Calculating Natural Optical Activity of Molecules from First Principles. *Annual Review of Physical Chemistry* **2017**, *68*, 399–420.

(3) Crawford, T. D. In *Frontiers of Quantum Chemistry*; Wójcik, M. J., Nakatsuji, H., Kirtman, B., Ozaki, Y., Eds.; Springer: Singapore, 2018; pp 49–68.

(4) Shavitt, I.; Bartlett, R. J. *Many-Body Methods in Chemistry and Physics: MBPT and Coupled-Cluster Theory*; University Press: Cambridge, 2009.

(5) Crawford, T. D.; Schaefer, H. F. In *Reviews in Computational Chemistry*; Lipkowitz, K., Boyd, D., Eds.; VCH Publishers: New York, 2000; Vol. 14; pp 33–136.

(6) Helgaker, T.; Coriani, S.; Jørgensen, P.; Kristensen, K.; Olsen, J.; Ruud, K. Recent Advances in Wave Function-Based Methods of Molecular-Property Calculations. *Chemical Reviews* **2012**, *112*, 543–631.

(7) Mach, T.; Crawford, T. Basis Set Dependence of Coupled Cluster Optical Rotation Computations. *J. Phys. Chem. A* **2011**, *115*, 10045–10051.

(8) Baranowska-Łączkowska, A.; Łączkowski, K. The ORP Basis Set Designed for Optical Rotation Calculations. *J. Comput. Chem.* **2013**, *34*, 2006–2013.

(9) Haghdani, S.; Astrand, P.; Koch, H. Optical Rotation from Coupled Cluster and Density Functional Theory: The Role of Basis Set Convergence. *J. Chem. Theory Comput.* **2016**, *12*, 535–548.

(10) Papajak, E.; Truhlar, D. G. Convergent Partially Augmented Basis Sets for Post-Hartree-Fock Calculations of Molecular Properties and Reaction Barrier Heights. *J. Chem. Theory Comput.* **2011**, *7*, 10–18.

(11) Baranowska, A.; Łączkowski, K.; Sadlej, A. J. Model Studies of the Optical Rotation, and Theoretical Determination of its Sign for β-Pinene and *trans*-Pinane. *J. Comput. Chem.* **2010**, *31*, 1176–1181.

(12) Wiberg, K. B.; Caricato, M.; Wang, Y.; Vaccaro, P. H. Towards the Accurate and Efficient Calculation of Optical Rotatory Dispersion Using Augmented Minimal Basis Sets. *Chirality* **2013**, *25*, 606–616.

(13) Ruud, K.; Taylor, P. R.; Åstrand, P. Zero-Point Vibrational Effects on Optical Rotation. *Chem. Phys. Lett.* **2001**, *337*, 217–223.

(14) Ruud, K.; Zanasi, R. The Importance of Molecular Vibrations: The Sign Change of the Optical Rotation of Methyloxirane. *Angew. Chem. Int. Ed.* **2005**, *44*, 3594–2596.

(15) Mort, B.; Autschbach, J. Magnitude of Zero-Point Vibrational Corrections to Optical Rotation in Rigid Organic Molecules: A Time-dependent Density Functional Study. *J. Phys. Chem. A* **2005**, *109*, 8617–8623.

(16) Kongsted, J.; Ruud, K. Solvent Effects on Zero-Point Vibrational Corrections to Optical Rotations and Nuclear Magnetic Resonance Shielding Constants. *Chem. Phys. Lett.* **2008**, *451*, 226–232.

(17) Pedersen, T. B.; Kongsted, J.; Crawford, T. D. Gas Phase Optical Rotation Calculated from Coupled Cluster Theory with Zero-Point Vibrational Corrections from Density Functional Theory. *Chirality* **2009**, *21*, E68–E75.

(18) Pedersen, T. B.; Kongsted, J.; Crawford, T. D.; Ruud, K. On the Importance of Vibrational Contributions to Small-angle Optical Rotation: Fluoro-oxirane in Gas Phase and Solution. *J. Chem. Phys.* **2009**, *130*, 034310.

(19) Wiberg, K. B.; Vaccaro, P. H.; Cheeseman, J. R. Conformational Effects on Optical Rotation. 3-Substituted 1-Butenes. *J. Am. Chem. Soc.* **2003**, *125*, 1888–1896.

(20) Wiberg, K. B.; Wang, Y.; Vaccaro, P. H.; Cheeseman, J. R.; Luderer, M. R. Conformational Effects on Optical Rotation. 2-Substituted Butanes. *J. Phys. Chem. A* **2005**, *109*, 3405–3410.

(21) Lambert, J.; Compton, R.; Crawford, T. D. The Optical Activity of Carvone: A Theoretical and Experimental Investigation. *J. Chem. Phys.* **2012**, *136*, 114512.

(22) Du, Y.; Pearce, K. C.; Dai, Y.; Krai, P.; Dalal, S.; Cassera, M. B.; Goetz, M.; Crawford, T. D.; Kingston, D. G. Antiplasmodial Sesquiterpenoid Lactones from *Trichospira verticillata*: Structure Elucidation by Spectroscopic Methods and Comparison of Experimental and Calculated ECD Data. *J. Nat. Prod.* **2017**, *80*, 1639–1647.

(23) Kumata, Y.; Furukawa, J.; Fueno, T. The Effect of Solvents on the Optical Rotation of Propylene Oxide. *Bull. Chem. Soc. Jpn.* **1970**, *43*, 3920–3921.

(24) Berova, N., Nakanishi, K., Woody, R., Eds. *Circular Dichroism: Principles an Applications*, 2nd ed.; Wiley: New York, 2000.

(25) Wilson, S. M.; Wiberg, K. B.; Cheeseman, J. R.; Frisch, M. J.; Vaccaro, P. H. Nonresonant Optical Activity of Isolated Organic Molecules. *J. Phys. Chem. A* **2005**, *109*, 11752–11764.

(26) Mukhopadhyay, P.; Zuber, G.; Goldsmith, M.; Wipf, P.; Beratan, D. N. Solvent Effect on Optical Rotation: A Case Study of Methyloxirane in Water. *ChemPhysChem* **2006**, *7*, 2483–2486.

(27) Mukhopadhyay, P.; Zuber, G.; Wipf, P.; Beratan, D. N. Contribution of a Solutes Chiral Solvent Imprint to Optical Rotation. *Angew. Chem. Int. Ed.* **2007**, *46*, 6450–6452.

(28) Miertuš, S.; Scrocco, E.; Tomasi, J. Electrostatic Interaction of a Solute with a Continuum - a Direct Utilization of Ab Initio Molecular Potentials for the Prevision of Solvent Effects. *Chem. Phys.* **1981**, *55*, 117–129.

(29) Tomasi, J.; Mennucci, B.; Cammi, R. Quantum Mechanical Continuum Solvation Models. *Chem. Rev.* **2005**, *105*, 2999–3093.

(30) Mennucci, B.; Tomasi, J.; Cammi, R.; Cheeseman, J.; Frisch, M.; Devlin, F.; Gabriel, S.; Stephens, P. Polarizable Continuum Model (PCM) Calculations of Solvent Effects on Optical Rotations of Chiral Molecules. *J. Phys. Chem. A* **2002**, *106*, 6102–6113.

(31) Lahiri, P.; Wiberg, K. B.; Vaccaro, P. H.; Caricato, M.; Crawford, T. D. Large Solvation Effect in the Optical Rotatory Dispersion of Norbornenone. *Angew. Chem. Int. Ed. Engl.* **2013**, *53*, 1386–1389.
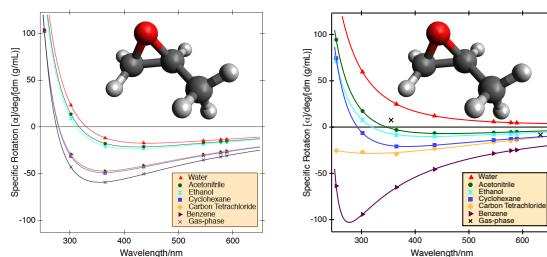
(32) Lipparini, F.; Egidi, F.; Cappelli, C.; Barone, V. The Optical Rotation of Methyloxirane in Aqueous Solution: A Never Ending Story. *J. Chem. Theory Comput.* **2013**, *9*, 1880–1884.

(33) Kongsted, J.; Pedersen, T. B.; Jensen, L.; Hansen, A. E.; Mikkelsen, K. V. Coupled Cluster and Density Functional Theory Studies of the Vibrational Contribution to the Optical Rotation of (*S*)-Propylene Oxide. *J. Am. Chem. Soc.* **2006**, *128*, 976–982.

(34) Fattebert, J. L.; Gygi, F. Density Functional Theory for Efficient Ab Initio Molecular Dynamics Simulations in Solution. *J. Comput. Chem.* **2002**, *23*, 662–666.

(35) Fattebert, J. L.; Gygi, F. First-Principles Molecular Dynamics Simulations in a Continuum Solvent. *Int. J. Quantum Chem.* **2003**, *93*, 139–147.

(36) Scherlis, D. A.; Fattebert, J. L.; Gygi, F.; Cococcioni, M.; Marzari, N. A Unified Electrostatic and Cavitation Model for First-Principles Molecular Dynamics in Solution. *J. Chem. Phys.* **2006**, *124*, 74103.

(37) Andreussi, O.; Dabo, I.; Marzari, N. Revised Self-Consistent Continuum Solvation in Electronic-Structure Calculations. *J. Chem. Phys.* **2012**, *136*, 064102.

(38) Dziedzic, J.; Helal, H. H.; Skylaris, C.-K.; Mostofi, A. A.; Payne, M. C. Minimal Parameter Implicit Solvent Model for Ab Initio Electronic-Structure Calculations. *EPL* **2011**, *95*, 43001.

(39) Dziedzic, J.; Fox, S. J.; Fox, T.; Tautermann, C. S.; Skylaris, C.-K. Large-scale DFT Calculations in Implicit Solvent - A Case Study on the T4 Lysozyme L99A/M102Q Protein. *Int. J. Quantum Chem.* **2013**, *113*, 771–785.

(40) Fox, S. J.; Dziedzic, J.; Fox, T.; Tautermann, C. S.; Skylaris, C.-K. Density Functional Theory Calculations on Entire Proteins for Free Energies of Binding: Application to a

Model Polar Binding Site. *Proteins-Structure Function and Bioinformatics* **2014**, *82*, 3335–3346.

(41) Womack, J. C.; Anton, L.; Dziedzic, J.; Hasnip, P. J.; Probert, M. I.; ; Skylaris, C. DL_MG: A Parallel Multigrid Poisson and Poisson-Boltzmann Solver for Electronic Structure Calculations in Vacuum and Solution. *J. Chem. Theory Comput.* **2018**, *14*, 1412–1432.

(42) Howard, J. C.; Womack, J. C.; Dziedzic, J.; Skylaris, C.-K.; Pritchard, B. P.; Crawford, T. D. Electronically Excited States in Solution via a Smooth Dielectric Model Combined with Equation-of-Motion Coupled Cluster Theory. *Journal of Chemical Theory and Computation* **2017**, *13*, 5572–5581.

(43) Lipparini, F.; Mennucci, B. Perspective: Polarizable Continuum Models for Quantum-Mechanical Descriptions. *J. Chem. Phys.* **2016**, *144*, 160901.

(44) Cammi, R. *Molecular Response Functions for the Polarizable Continuum Model*; SpringerBriefs in Molecular Science; Springer: Cham, 2013.

(45) Caricato, M. Implementation of the CCSD-PCM Linear Response Function for Frequency Dependent Properties in Solution: Application to Polarizability and Specific Rotation. *J. Chem. Phys.* **2013**, *139*, 114103.

(46) Kendall, R. A.; Dunning, T. H.; Harrison, R. J. Electron-Affinities of the 1st-Row Atoms Revisited - Systematic Basis-Sets and Wave-Functions. *J. Chem. Phys.* **1992**, *96*, 6796–6806.

(47) Pedersen, T. B.; Koch, H.; Boman, L.; Sánchez de Merás, A. M. Origin Invariant Calculation of Optical Rotation Without Recourse to London Orbitals. *Chem. Phys. Lett.* **2004**, *393*, 319–326.

(48) Krishnan, R.; Binkley, J. S.; Seeger, R.; Pople, J. A. Self-consistent Molecular Orbital Methods. XX. A Basis Set for Correlated Wave Functions. *J. Chem. Phys.* **1980**, *72*, ,650–654.

(49) Frisch, M. J.; Trucks, G. W.; Schlegel, H. B.; Scuseria, G. E.; Robb, M. A.; Cheeseman, J. R.; Scalmani, G.; Barone, V.; Mennucci, B.; Petersson, G. A. et al. Gaussian09 Revision E.01. Gaussian Inc. Wallingford CT 2009.

(50) Parrish, R. M.; Burns, L. A.; Smith, D. G. A.; Simmonett, A. C.; DePrince, A. E.; Hohenstein, E. G.; Bozkaya, U.; Sokolov, A. Y.; Di Remigio, R.; Richard, R. M. et al. Psi4 1.1: An Open-Source Electronic Structure Program Emphasizing Automation, Advanced Libraries, and Interoperability. *Journal of Chemical Theory and Computation* **2017**, *13*, 3185–3197.

(51) PCMSolver. https://doi.org/10.5281/zenodo.1187000.

(52) Becke, A. D. Density-Functional Thermochemistry. III. The Role of Exact Exchange. *J. Chem. Phys.* **1993**, *98*, 5648–5652.

(53) Lee, C. T.; Yang, W. T.; Parr, R. G. Development of the Colle-Salvetti Correlation-Energy Formula into a Functional of the Electron-Density. *Phys. Rev. B* **1988**, *37*, 785–789.

(54) Stephens, P. J.; Devlin, F. J.; Chabalowski, C. F.; Frisch, M. J. Ab-Initio Calculation of Vibrational Absorption and Circular-Dichroism Spectra Using Density-Functional Force-Fields. *J. Phys. Chem.* **1994**, *98*, 11623–11627.

(55) Kongsted, J.; Pedersen, T. B.; Strange, M.; Osted, A.; Hansen, A. E.; Mikkelsen, K. V.; Pawlowski, F.; Jørgensen, P.; Hättig, C. Coupled Cluster Calculations of the Optical Rotation of *S*-propylene Oxide in Gas Phase and Solution. *Chem. Phys. Lett.* **2005**, *401*, 385–392.

(56) Christiansen, O.; Mikkelsen, K. V. Coupled Cluster Response Theory for Solvated Molecules in Equilibrium and Nonequilibrium Solvation. *J. Chem. Phys.* **1999**, *110*, 8348–8360.

(57) Stephens, P. J.; Devlin, F. J.; Cheeseman, J. R.; Frisch, M. J. Calculation of Optical Rotation Using Density Functional Theory. *J. Phys. Chem. A* **2001**, *105*, 5356–5371.

(58) Ruud, K.; Stephens, P. J.; Devlin, F. J.; Taylor, P. R.; Cheeseman, J. R.; Frisch, M. J. Coupled-Cluster Calculations of Optical Rotation. *Chem. Phys. Lett.* **2003**, *373*, 606 – 614.

(59) Moore, B.; Srebro, M.; Autschbach, J. Analysis of Optical Activity in Terms of BOnds and Lone-Pairs: The Exceptionally Large Optical Rotation of Norbornenone. *J. Chem. Theory Comput.* **2012**, *8*, 4336–4346.

(60) Caricato, M.; Vaccaro, P. H.; Crawford, T. D.; Wiberg, K. B.; Lahiri, P. Insights on the Origin of the Unusualy Large Specific Rotation of (1S,4S)-Norbornenone. *J. Phys. Chem. A* **2014**, *118*, 4863–4871.

(61) Aharon, T.; Lemler, P.; Vaccaro, P. H.; Caricato, M. Comparison of Measured and Predicted Specific Optical Rotation in Gas and Solution Phases: A Test for the Polarizable Continuum Model of Solvation. *Chirality* **2018**, *30*, 1–13.

(62) Crawford, T. D.; Kumar, A.; Hannon, K. P.; Höfener, S.; Visscher, L. Frozen-Density Embedding Potentials and Chiroptical Properties. *J. Chem. Theory Comput.* **2015**, *11*, 5305–5315.

(63) Caricato, M. Linear Response Coupled Cluster Theory with the Polarizable Continuum Model Within the Singles Approximation for the Solvent Response. *J. Chem. Phys.* **2018**, *148*, 134113.

TOC Graphic

Calculating Optical Rotatory Dispersion Spectra in Solution Using a Smooth Dielectric Model

J. Coleman Howard and T. Daniel Crawford